6.3 A COMBINED RADAR-RADIOMETER ALGORITHM TO ESTIMATE HYDROMETEOR PROFILES IN TROPICAL CYCLONES

Haiyan Jiang* and Edward J. Zipser
Department of Meteorology, University of Utah, Salt Lake City, UT

1. INTRODUCTION

A better understanding of ice water content (IWC) and liquid water content (LWC) is important to improve our knowledge of cloud and precipitation processes and to validate microphysical schemes in numerical simulation models. The latent heat release in clouds provides energy and produces a warm-core structure, which is essential for development and maintenance of the circulation of the storm. However, IWC and LWC have implications on both dynamical and microphysical processes within tropical cyclone. At the advent of the Tropical Rainfall Measuring Mission (TRMM) during 1997, the remote sensing measurements from both radar and radiometer provide a very powerful tool to estimate hydrometeor profiles in tropical precipitation systems. To improve understanding of tropical cyclone development, motion, intensification, and landfalling impacts, the cooperative NASA/NOAA aircraft-based field programs into tropical cyclones (CAMEX-3, 4) were performed in 1998 and 2001. The Doppler radar on the NASA ER-2 airplane (EDOP) and Advanced Microwave Precipitation Radiometer (AMPR) also on the ER-2 during CAMEX have wavelengths close to those of TRMM.

The microwave remote sensing techniques for the estimation of precipitation have advanced considerably over the last decade due to both observational and radiative transfer modeling studies. The “emission”-based algorithms are based on the lower frequency and the emission/absorption effect by raindrops (Wilheit et al. 1991). These physical methods derive a simple relationship between observed brightness temperatures and the surface rain rate by assuming some type of hypothetical hydrometeor profile. Observational and modeling studies have shown that passive microwave measurements of precipitating clouds are sensitive to many aspects of the vertical distribution of various hydrometeor species and not only the surface rain rate. Profiling algorithms are designed to use all the available channels and both emission and scattering characteristics of cloud and precipitation particles. The vertical hydrometeor profiles can be retrieved by various inversion techniques. An iterative scheme was used by Kummerow et al. (1989) to match the observed brightness temperatures with those simulated from a relatively small number of specified profiles. Since there are typically multiple distinct profiles that can satisfy a small set of observations, other information about the vertical distribution of hydrometeors is needed to constrain the retrieval. The database of cloud model-derived profiles has been used extensively in many Bayesian retrieval methods (Kummerow et al. 1996; Mugnai et al. 1993). The success of these algorithms is influenced by the problems of cloud model microphysical information. Marzano et al. (1999) showed that the opportunities to estimate hydrometeor profiles and cloud characteristics improve by combining radar and radiometers.

The combined radar-radiometer profile-retrieval algorithm developed here uses radar reflectivity derived hydrometeor profiles as input to a forward radiative transfer model to retrieve the profiles of ice and liquid precipitation contents by minimizing the differences between observed brightness temperatures and simulated ones iteratively. The purpose of this paper is to implement and test this combined radar-radiometer profiling algorithm by applying it to EDOP and AMPR tropical cyclone datasets during CAMEX. The advantage of airborne AMPR and EDOP data is that they have a higher surface resolution than TRMM sensors, which would average the signals from adjacent convective elements. Applications of the algorithm to TRMM Microwave Imager and Precipitation Radar observations will be the subject of a future investigation by the authors.

2. DATASETS

The Advanced Microwave Precipitation Radiometer (AMPR) is a four channel scanning passive microwave radiometer measuring fully or partially polarized radiation at 10.7, 19.35, 37.1, and 85.5 GHz. The antenna beamwidths are 8^0, 8^0, 4.2^0, 1.8^0 for the 10.7, 19.35, 37.1, and 85.5 GHz channels, respectively. A full description of the AMPR instrument can be found in Spencer et al. (1994). The NASA ER-2 Doppler radar (EDOP) is an X-band (9.6 GHz) Doppler radar with fixed nadir and forward pointing beams with a beam width of 2.9°. It can map out the reflectivities and Doppler winds in the vertical plane along the aircraft path (Heymsfield et al., 1996). An X-band radar suffers from attenuation problem, especially in intensive convective precipitations. The EDOP attenuation correction is performed by using a combined Hitschfeld-Bordan and surface reference technique (Tian et al., 2002).

To facilitate collocation of passive and active microwave measurements from the AMPR and EDOP, both of which fly on the NASA ER-2 aircraft at 20 km altitude, only the nadir-view data from these instruments are considered. At nadir, the AMPR measurements represent an equal mix of horizontal and vertical polarization. The AMPR nadir ground resolutions are 2.8

* *Corresponding author address*: Haiyan Jiang, Dept. of Meteorology, Univ. of Utah, Salt Lake City, UT 84112; e-mail: hjiang@met.utah.edu

km, 2.8 km, 1.5 km, and 0.6 km for the four channels, respectively. Nadir observations from the EDOP have a surface footprint of approximately 1.0 km. A "nearest neighbor" interpolation is used for collocating observations from two sensors.

A precipitation classification algorithm is developed to separate stratiform/convective regimes by using EDOP reflectivity and Doppler velocity measurements. This algorithm is modified from Gerry Heymsfield's (personal communication) classification by adding a 3 m/s Doppler upward wind criterion to define convective region (Lang et al. 2003). For the rest, a Gaussian fit is used to identify the bright band. Profiles with bright band and the maximum EDOP reflectivity at 1-3 km less than 45 dBZ are set to stratiform regime. Profiles without a bright band, and with maximum EDOP reflectivity anywhere from 1-3 km or 6-10 km greater than 45 dBZ are set to convective regime. All other rain regions are set to intermediate class.

3. RETRIEVAL METHOD

The retrieval algorithm uses both radar and radiometer observations in the retrieval process. A radiative transfer model is needed to calculate the microwave upwelling brightness temperature. Input fields to the radiative transfer model are built from various hurricane data sources. Initial hydrometeor profiles are estimated from radar reflectivity Ze measurements by using a Ze-water content relatioship derived from the exponential drop size distribution (DSD). An iterative inversion is performed to retrieve the hydrometeor profiles by minimizing the difference between observed and simulated brightness temperatures.

a. RTM

The original radiative transfer model (RTM) used here was described by Kummerow et al. (1996). It is based on the Eddington approximation for a multi-layered plane parallel medium. The mean error of this Eddington approximation relative to a Monte Carlo scheme model is about 2.7 K (1.2 K) at 85 GHz (19 GHz) and can reach 12 K (5.3 K) in very strong precipitation (Viltard et al. 1998). However, this type of model is easy to operate and fast.

This RTM allows for six hydrometeor types (e.g., cloud ice, cloud liquid water, rain water, snow, graupel, and hail). In this application to hurricanes, only 4 hydrometeor types (e.g., cloud liquid water, rain water, snow, and graupel) are considered. The cloud ice is not taken into account because of its negligible influence in most cases (Viltard et al. 1998). And hail is very rare in hurricanes. This RTM takes into account ocean surface emission, cosmic background radiation, atmospheric absorption by molecular oxygen and water vapor, absorption by cloud liquid water, and both absorption and scattering by liquid drops and ice particles.

b. Input data and hydrometeor content calculations

The RTM needs the input atmospheric parameters for the computation of the brightness temperatures. First, the temperature and humidity profiles are determined using the data from dropwindsondes from the ER-2 or DC-8. Second, the surface wind field is obtained from the NOAA Hurricane Research Division's hurricane surface wind analysis. Third, the mean SST is chosen also based on dropsonde data.

In the RTM, the cloud liquid water distribution is assumed to be mono-disperse. The distributions of rain, snow, and graupel are assumed to follow an exponential shape of the form $N(D) = N_0 e^{-\lambda D}$, where D is the diameter of the particles. Substituting this distribution to definition equations of water contents M_x (x represents different species, e. g., rain, snow, and graupel) and radar reflectivity Ze and integrating from zero to infinite particle diameter, we got a $Ze - M_x$ relationship as follow:

$$Ze = 720 N_{0x}{}^{-0.75} (\pi\rho_x)^{-1.75} M_x{}^{1.75} \qquad (1)$$

where ρ is density. We choose a density of 1.0 g/cm^3 for rain, 0.1 g/cm^3 for snow, and 0.4 g/cm^3 for graupel. Then we can see that above $Ze - M_x$ relation is only N_0-dependent. In this retrieval, we input EDOP Ze profiles to the RTM and iteratively adjust N_0's for rain, snow, and graupel respectively by minimizing the difference between observed and simulated brightness temperatures. Notice that N_0 is assumed to be constant for any individual vertical profile in all layers. The initial values of N_0 are 2.2x10^7 m^{-4} for rain, 10^8 m^{-4} for snow, and 4x10^6 m^{-4} for graupel. The cloud liquid water content is assumed to be 10% of the rain water content (Tesmer and Wilheit, 1998).

Rain, snow, and graupel fraction profiles are needed to convert radar reflectivity profile into hydrometeor content profiles. In this preliminary test, we build fraction profiles based on the result of hurricane cloud model simulation by Lord et al. (1984, see their Fig. 6). A 100% rain water is assumed below the bottom of the melting layer. Graupel reaches its maximum at 6 km, and snow reaches its maximum at 12 km. A linear interpolation is used to set the fraction of rain and graupel within the melting layer, and to set the fraction of snow and graupel beyond their maximums. The freezing level is found based on radar bright band height. The top (bottom) of the melting layer is 500 m for stratiform and 750 m for convective/intermediate regime above (below) the freezing level. More tests could be done by assuming the rain, snow, and graupel fraction profiles for different rain types based on recent microphysical measurements in field programs.

c. Inversion

As previously mentioned, the inversion means that we iteratively look for the set of atmospheric characteristics (e.g., N_0 for rain, snow, and graupel respectively) that leads the RTM to calculate simulated

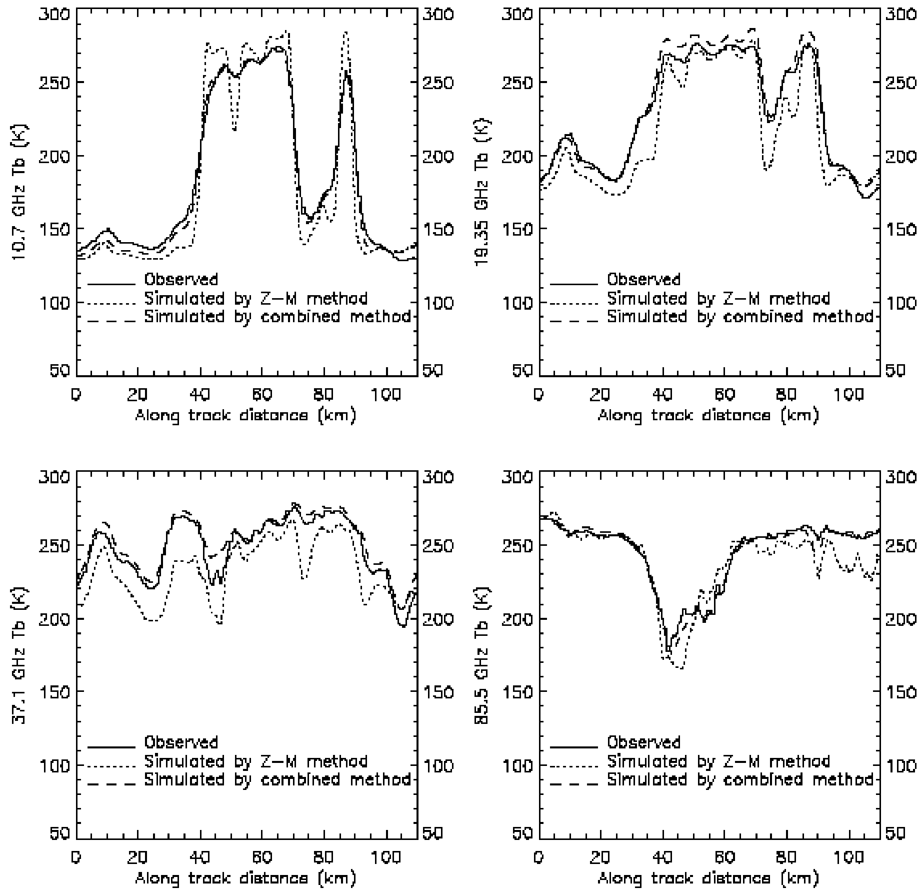

Figure 1. Comparison of observed brightness temperatures and simulated ones by Z-M method and radar/radiometer combined method at 10 (upper right), 19 (upper left), 37 (lower right), and 85 (lower left) GHz frequencies.

brightness temperatures as closely as possible to the observed ones. The inversion is done iteratively from the initial values. At each iteration, the error function is defined by the sum of the squares of errors in 4 channels.

We look for the minimum of the error function numerically. Convergence can be reached quickly for any strong rain region (convective or stratiform region), especially for the 10 and 85 GHz channels. For anvil and warm rain regions, there are some difficulties to get convergence for 19 and 37 GHz brightness temperatures.

4. RESULTS

The CAMEX-4 experiment was based in Florida to study tropical cyclones. Among the whole observation set of the CAMEX-4, one of the Tropical Storm Humberto flight pass during 19:32-19:40 on September 22, 2001 was selected because it contains well-sampled convective/ stratiform precipitations and all kind of RTM input data sources are available.

For comparison with this retrieval, the ice water content (IWC) and liquid water content (LWC) profiles are also calculated by applying empirical Z-M relations to EDOP reflectivity measurements, in which Z-IWC relationship is from Black (1990) and Z-LWC from Gamache et al. 1993 (therefore Z-M method).

Fig. 1 shows the comparison of AMPR observed brightness temperatures at 10, 19, 37, and 85 GHz and the output of those brightness temperatures from our combined radar/radiometer inversion algorithm and from the simulation by using Z-M method derived hydrometeor profiles (rain, snow, graupel fraction profiles are assumed as same as described in section 3(a)) as input to the RTM. It is obvious that the curves simulated by the combined algorithm are closer to AMPR observed ones relative to those simulated by Z-M method. This is an encouraging result.

Fig. 2 shows the comparisons of liquid water path (LWP) and ice water path (IWP) between the combined algorithm and Z-M method for this pass. Generally, the shapes of LWP and IWP curves calculated from these two methods are in phase. Although the total ice masses estimated by these two methods are in good agreement, the total liquid water mass estimated by Z-M method is smaller than that by the combined algorithm. This may show that the Z-LWC relation used here is not suitable for the microphysics in this case.

The mean water content profiles from combined radar/radiometer algorithm and from Z-M method for this Humberto pass are given in Fig. 3. Again, in an average sense, a good agreement between the new algorithm and Black (1990)'s Z-IWC relationship can be seen in ice regions. But in rain region, Z-LWC relation produces underestimates by a factor of 2 relative to the combined algorithm.

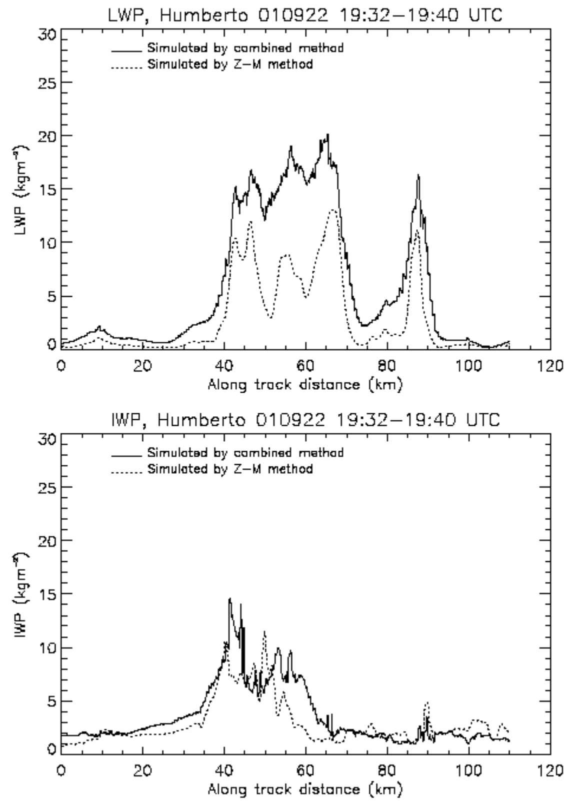

Figure 2. Liquid water path (LWP, upper) and ice water path (IWP, lower) calculated by the radar/radiometer combined method and Z-M method.

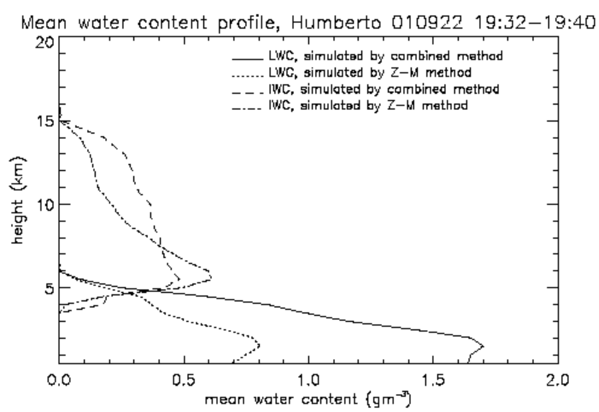

Figure 3. Mean water content profiles calculated by Z-M method and radar/radiometer combined method.

5. CONCLUSIONS AND FUTURE WORK

A combined radar/radiometer algorithm for retrieving hydrometeor content profiles in hurricanes is developed and tested by aircraft hurricane data. The good agreement between observed and simulated brightness temperatures shows that this inversion technique has promise. We are encouraged by similar good results for another 20-minutes pass in hurricane Humberto on 23 September.

Future work will focus on validating the retrieval results by using microphysics measurements, improving the assumption of rain, snow, and graupel fraction profiles by combining observations and 3D cloud model simulation results, and applying the new algorithm into TRMM satellite data**.**

6. REFERENCES

Black, R. A., 1990: Radar reflectivity-ice water content relationships for use above the melting level in hurricanes. *J. Appl. Meteor.*, **29**, 955-961.

Gamache, J. F., R. A. Houze, Jr., and F. D. Marks, Jr., 1993: Dual-aircraft investigation of the inner core of Hurricane Norbert. Part III: Water Budget. *J. Atmos.Sci.*, **50**, 3221-3243.

Heymsfield, G. M., and coauthors, 1996: The EDOP Radar System on the High-Altitude NASA ER-2 Aircraft. *J. Atmos.Oceanic Technol.,* **13**, 795–809.

Kummerow, C., R. A. Mack, and I. M. Hakkarinen, 1989: A Self-Consistency Approach to Improve Microwave Rainfall Rate Estimation from Space. *J. Appl. Meteor,*: **28**, 869–884.

Kummerow, C., W. S. Olson, and L. Giglio, 1996: A simplified scheme for obtaining precipitation and vertical hydometeor profiles from passive microwave sensors. *IEEE Trans. Geosci. Remote Sens.*, **34**, 1213-1232.

Lang, S., W.-K. Tao, J. Simpson, and B. Ferrier, 2003: Modeling of convective-stratiform precipitation processes: sensitivity to partitioning methods. *J. Appl. Meteor.*, 4**2,** 505-527.

Lord, S. J., H. E. Willoughby, and J. M. Piotrowicz, 1984: Role of a Parameterized Ice-Phase Microphysics in an Axisymmetric, Nonhydrostatic Tropical Cyclone Model. *J. Atmos. Sci.,* 41, **19**, 2836–2848.

Marzano, F. S., A. Mugnai, G. Panegrossi, N. Pierdicca, E. A. Smith, and J. Turk, 1999: Bayesian estimation of precipitating cloud parameters from combined measurements of spaceborne microwave radiometer and radar. *IEEE Trans. Geosci. Remote Sens.*, **37**, 596-613.

Mugnai, A., E. A. Smith, G. J. Tripoli, 1993: Foundations for Statistical–Physical Precipitation Retrieval from Passive Microwave Satellite Measurements. Part II: Emission-Source and Generalized Weighting-Function Properties of a Time-dependent Cloud-Radiation Model. *J. Appl. Meteor.,* **32**, 17–39.

Spencer, R. W., H. M. Goodman, and R. E. Hood, 1989: Precipitation retrieval over land and ocean with the SSM/I: Identification and characteristics of the scattering signal. *J. Atmos. Oceanic Technol.,* **6,** 254-273.

Tesmer, J. R., and T. T. Wilheit, 1998: An Improved Microwave Radiative Transfer Model for Tropical Oceanic Precipitation. *J.Atmos. Sci.,* **55**, 1674–1689.

Tian, L., G. M. Heymsfield, R. C. Srivastava, 2002: Measurement of Attenuation with Airborne and Ground-Based Radar in Convective Storms over Land and Its Microphysical Implications. *J. Appl. Meteor.*, **41**, 716–733.

Viltard, N., E. Obligis, V. Marecal, C. Klapisz, 1998: Retrieval of Precipitation from Microwave Airborne Sensors during TOGA COARE. *J. Appl. Meteor.*, **37**, 701–717.

Wilheit, T. T., A. T. C. Chang, and L. S. Chiu, 1991: Retrieval of Monthly Rainfall Indices from Microwave Radiometric Measurements Using Probability Distribution Functions. *J. Atmos. Oceanic Technol.* **8**, 118–136.